Measurement of Specific Heat Capacity and Electrical Resistivity of Industrial Alloys Using Pulse Heating Techniques

D. Basak,[1,2] **R. A. Overfelt,**[3] **and D. Wang**[3]

The determination of the specific heat capacity and electrical resistivity of Inconel 718, Ti-6Al-4V, and CF8M stainless steel, from room temperature to near the melting temperatures of the alloys, is described. The method is based on rapid resistive self-heating of a solid cylindrical specimen by the passage of a short-duration electric current pulse through it while simultaneously measuring the pertinent experimental quantities (i.e., voltage drop, current, and specimen temperature). From room temperature to about 1300 K, the properties are measured using an intermediate-temperature pulse-heating system by supplying a constant current from a programmable power supply and measuring the temperature using a Pt-Pt:13% Rh thermocouple welded to the surface of the specimen. From 1350 K to near the melting temperatures of the alloys, the properties are measured using a millisecond-resolution high-temperature pulse-heating system by supplying the current from a set of batteries controlled by a fast-response switching system and measuring the temperature using a high-speed pyrometer in conjunction with an ellipsometer, which is used to measure the corresponding spectral emissivity. The present study extends the application of these techniques, previously applied only to pure metals, to industrial alloys.

KEY WORDS: CF8M stainless steel; electrical resistivity; Inconel 718; pulse heating; specific heat capacity; Ti-6Al-4V.

1. INTRODUCTION

Accurate and precise data on the thermophysical properties of pure metals and alloys are becoming increasingly important for the scientific understanding

---
[1] Metallurgy Division, National Institute of Standards and Technology, Gaithersburg, Maryland 20899, U.S.A.

[2] To whom correspondence should be addressed. E-mail: basis@nist.gov

[3] Mechanical Engineering Department, Auburn University, Auburn, Alabama 36849, U.S.A.

of a number of metallurgical phenomena as well as improved design of material processes for efficient and cost-effective manufacture of production components. Data are needed for solid materials over wide ranges of temperatures and also for molten materials up to about 150 K into the liquid phase. Many of these materials are complex multicomponent alloys, exhibiting high melting temperatures, and can react appreciably with ceramic crucibles used to contain them while molten.

Unfortunately, there have been few reports of such data for complex alloys due to the experimental difficulties involved. Thus, containerless methods, as reviewed by Egry et al. [1] and Bakhtiyarov and Overfelt [2], and *semi*-containerless methods are under development to enable reliable measurements and to minimize contamination from extraneous reactions. In the present paper, we review a semi-containerless method for measurements of the specific heat capacity and electrical resistivity of solid metal alloys using millisecond-resolution resistive pulse heating. In addition, we extend the application of the method to three important industrial alloys, Inconel 718, Ti-6Al-4V, and CF8M stainless steel, from room temperature to near their solidus temperatures. Data for the electrical resistivity are compared to theoretical estimates based on separate measurements of the thermal conductivity of the alloys, where available, using the Wiedemann–Franz–Lorenz (W-F-L) law.

2. MEASUREMENT METHOD

The National Institute of Standards and Technology (NIST) millisecond-resolution pulse-heating system and the University of Tennessee (UT) pulse-heating calorimeter were used to determine the properties of three alloys from room temperature to near their melting temperatures. The NIST system uses a current pulse of sub-second duration, while the UT system employs a pulse longer than 1 s.

2.1. High-Temperature Pulse-Heating System

The high-temperature pulse-heating method is based on rapid resistive self-heating of the specimen from room temperature to high temperatures (up to near its melting temperature) in sub-second duration by the passage of an electric current pulse through it. Eight experimental quantities are recorded with the high-speed data acquisition system with a sampling rate of 4 kHz, during the heating period only. Acquiring data during cooling is not necessary with this technique. Two pyrometer outputs were recorded at 625 and 651 nm, with bandwidths of 54 and 34 nm, respectively. Polarimeter voltage outputs from the four detectors were recorded. The voltage drop

across the standard resistor in series with the specimen and the voltage drop across the spring-loaded knife-edges that impinge on the specimen were also recorded. The current through the specimen is determined from the voltage drop across a standard resistor.

The normal spectral emissivity is measured with a high-speed laser polarimeter [3]. In this method, the normal spectral emissivity is determined by directing a modulated and polarized beam from a helium-neon laser ($\lambda = 633$ nm) to the specimen and analyzing the polarization state of the reflected beam. The surface radiance temperature of the specimen is measured at two wavelengths, 625 and 651 nm, by two high-speed solid-state optical pyrometers [4, 5], each focussed on a region diametrically opposite to the other on the specimen surface. These two wavelengths bracket the operating wavelength of the laser source. The surface radiance temperature of the specimen at 633 nm is calculated by linear interpolation of the surface radiance temperatures measured at the bracketing wavelengths. Using Planck's law, the true temperature of the specimen is then determined from the data on radiance temperature and normal spectral emissivity, both at 633 nm. The use of an interpolated radiance temperature at 633 nm rather than the actual value results in an error of less than 1 K.

The hemispherical total emissivity of the specimen was determined from several steady-state experiments, which were used to compute the radiation loss from the specimen during heating. This system was used along with a PID (proportional-integral-derivative) control program to isothermally hold the specimen during the steady-state experiments.

2.2. Intermediate-Temperature Pulse-Heating System

The intermediate-temperature pulse calorimeter also uses the concept of resistive self-heating but employs a longer current pulse, typically lasting for 6 to 8 s. A programmable power supply is used, instead of a battery bank, which is triggered by the control computer using a dc signal to send a specified constant current for a specified length of time to form the pulse. The power supply is in series with a $0.01\ \Omega$ standard resistor and the specimen. The three transient signals acquired during heating are the voltage across the effective specimen length, the current through the specimen, and the thermoelectric voltage from the thermocouple welded to the surface of the specimen. These electrical signals are measured as a function of time and are sent through amplifiers and a set of A/D converters before being recorded on a personal computer. The voltage taps, made out of 0.25 mm diameter nickel wires, are spot-welded to the specimen with a separation of about 4 cm. The current is measured from the voltage drop across the standard resistor. A Pt-Pt:13% Rh (type-R) thermocouple, 0.125 mm in

diameter, was spot welded to the center of the specimen to measure the thermoelectric voltage.

The distance between the voltage taps is measured precisely with a knife-edge device calibrated with a traversing microscope. This distance defines the effective specimen length used in the energy balance equation. A small current, e.g., 10 A, is passed through the specimen, and the voltage drop across the voltage taps and the knife edges is measured. The distance between the voltage taps is calculated from the ratio of the voltage drops between the voltage taps and the knife edges which is the same as the ratio of the distance between them. The design of the original measurement system and the methods of measuring the experimental quantities are provided in earlier publications [6, 7].

3. MEASUREMENTS

The materials investigated were metal alloys, Inconel 718, Ti-6Al-4V, and CF8M stainless steel of the compositions shown in Table I. Samples of these alloys were machined from investment cast bars.

Measurements were performed on cylindrical specimens that were first polished to a smooth finish (down to 600-grit silicon carbide paper) to provide good reflection characteristics for the laser beam and to minimize the radiation losses at high temperatures. Before the actual experiments were commenced, the specimen surface was cleaned by providing a preheat-pulse to around 1400 K in vacuum and holding it at this temperature for approximately 1 s, to remove any contaminants from the surface and relieve any internal stresses. This treatment was the same for all the samples used in both systems.

3.1. High-Temperature Pulse-Heating System

Before the transient experiments, several brief steady-state experiments were performed between 1300 K to near the melting temperature of the

Table I. Compositions of Sample Materials

Alloy	Element (mass%)											
	Ni	Fe	Co	Cr	Ti	Mo	Nb	Cu	Si	Mn	Al	V
IN 718	balance	18.9		18.3	0.83	2.0	4.6					
CF8M	10.28	balance	0.15	18.3	0.83	2.5	4.6	0.31	1.42	0.99		
Ti-6Al-4V				balance							6	4

alloys to compute the hemispherical total emissivity of the specimen before conducting the specific heat experiments with the high-temperature system. The details of this technique are discussed in an earlier publication [8]. During the steady-state period the power input to the specimen is equal to the power radiated by it, as given by the following equation,

$$EI = \varepsilon_T \sigma A_s (T^4 - T_0^4) \qquad (1)$$

where E is the voltage across the effective specimen, I is the current through the specimen, ε_T is the hemispherical total emissivity, σ is the Stephan–Boltzmann constant, A_s is the surface area of the effective specimen, T is the specimen absolute temperature, and T_0 is the ambient absolute temperature. The only unknown quantity in Eq. (1) is ε_T, which is then determined. Similar experiments were repeated at intervals of 100 K and a function of ε_T versus temperature was obtained. This function was used in the specific heat equation to compute the power loss from the specimen during the pulse experiments performed above 1300 K.

The solidus temperatures of the alloys, IN 718, Ti-6Al-4V, and CF8M stainless steel, are 1420, 1943, and 1550 K, respectively [9, 10]. Specimens were heated from room temperature to near the solidus temperatures in about 200 ms. The average current used was about 400 A. The specimen was heated in a sealed chamber back-filled with argon at slightly above atmospheric pressure.

3.2. Intermediate-Temperature Pulse-Heating System

For the measurements performed with the intermediate-temperature pulse-heating system, the power loss is computed using a method different from that used for the high-temperature system. The power loss was computed from the slope of the temperature-versus-time data recorded during cooling and then subtracted from the heating rate at each recorded temperature. It is assumed that at any given temperature the specimen is in the same physical state during heating as during cooling.

Specimens were heated from room temperature to approximately 1300 K in about 6 s, thus at an average heating rate of about $165 \, \text{K} \cdot \text{s}^{-1}$. The cooling period extended for about 12 min, the average cooling rate being less than $2 \, \text{K} \cdot \text{s}^{-1}$. The three experimental quantities were recorded with a time resolution of about 50 ms during the heating period and with a resolution of 1 s during the subsequent cooling period. The voltage, current, and the thermoelectric voltage from a type-R thermocouple were amplified and recorded.

4. RESULTS AND DISCUSSION

Details of the determination of specific heat capacity from pulse heating experiments are discussed in earlier publications [6, 11]. The specific-heat-capacity data for the alloys were obtained from the voltage, current, and temperature by equating the power input to the specimen to the sum of the power absorbed and the power lost. The electrical resistivity was calculated from the voltage and current data recorded during the experiments. Intermediate-temperature and high-temperature results are plotted in separate graphs for better resolution in the two temperature ranges. The agreement above and below ~ 1300 K may not be very good for some alloys. This is mainly due to two reasons. Some of the alloys have structural changes near this temperature which affect the slope of the specific heat capacity. Also, heat capacity data are rate dependent, and the rates of heating vary considerably for these two measurement systems. Some of these issues are discussed in more detail later in this section.

4.1. Specific Heat Capacity

Figure 1 shows the specific heat capacity in the approximate temperature range from 400 to 1250 K, determined by using the intermediate temperature pulse-heating system, for the three alloys, IN 718, Ti-6Al-4V, and CF8M stainless steel. When available, the data are compared to the data from recent differential scanning calorimeter (DSC) experiments [9].

As with many multicomponent alloys, the specific heat capacity and the electrical resistivity are sensitive to thermal history prior to the experiments. The specific heat capacity of materials measured by continuous heating depends not only on the intrinsic ability of the material to absorb energy but also on the energy absorption and release during any structural phase changes. The latter is more sensitive to heating rate effects and the state of the material prior to heating. Hence, materials undergoing such changes during the heating process will show a deviation from a smooth curve as is observed with IN 718 in the temperature range 940 to 1040 K. For samples of this alloy pre-heated to 1400 K, the room-temperature microstructure should consist of γ (FCC) with a small amount of γ' and γ'' in the grain boundaries. Solubility of these phases in γ is temperature dependent. As the temperature increases during pulse-heating, some of the precipitates are expected to dissolve around 900 K giving rise to the sharp increase in specific heat capacity, until around 1040 K where the effects due to the specific heat and structural changes balance out. These transformations have been discussed in more detail by Brooks et al. [12]. Specific-heat-capacity data from the Auburn University Thermophysical Properties
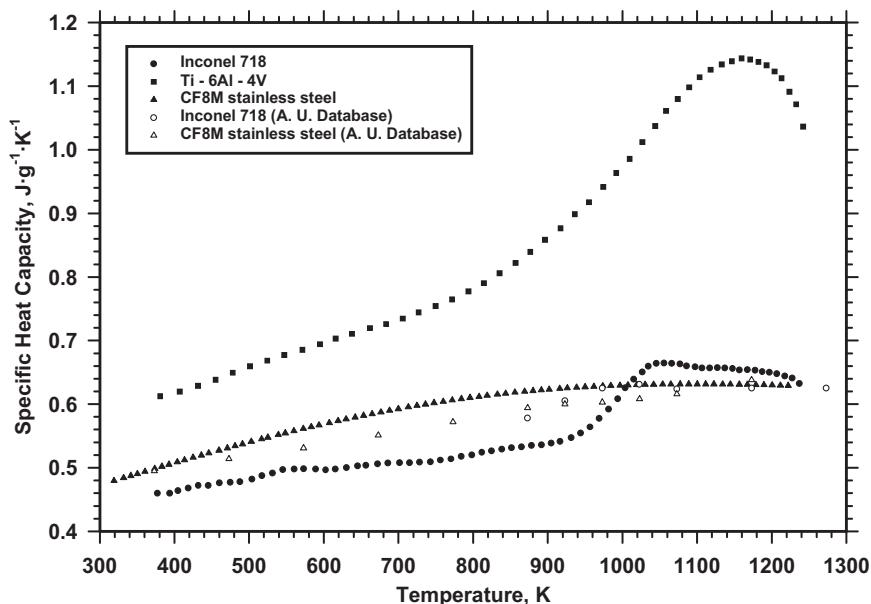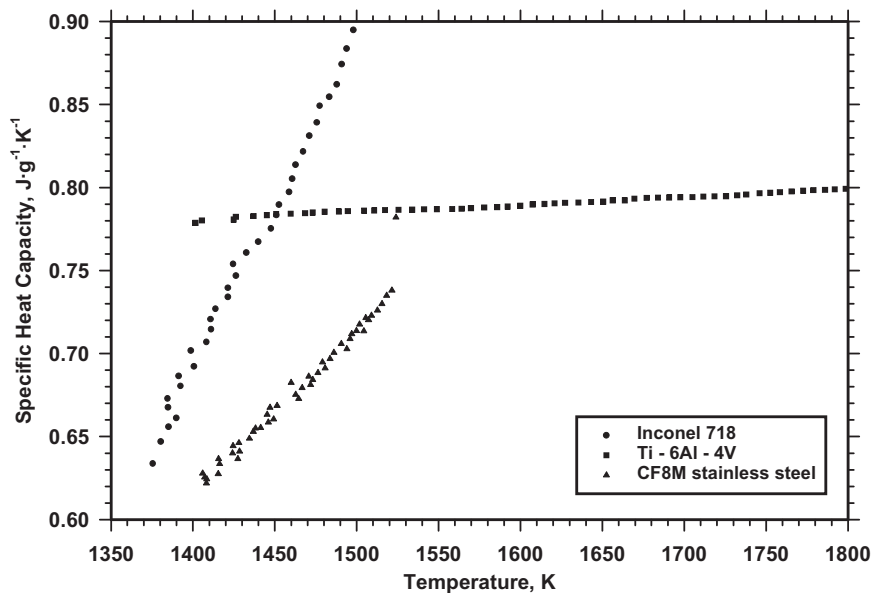
Fig. 1. Specific heat capacity versus temperature for Inconel 718, Ti-6Al-4V, and CF8M stainless steel, measured with the intermediate-temperature pulse-heating system. Filled symbols represent data from current work. Open symbols represent data from the Auburn University thermophysical properties database [10].

Database [9] are shown (open symbols) alongside the data from the current work, in the temperature range of availability. They have similar trends; the differences are due to the fact that the literature data have been measured with a differential scanning calorimeter (DSC) at much lower heating rates ($20 \ K \cdot min^{-1}$).

The specific heat capacity for the alloy, Ti-6Al-4V, determined with the intermediate-temperature pulse-heating system (Fig. 1) shows an initial gradual increase with temperature and a subsequent increase in the slope up to around 1160 K, where a peak in the data is observed. This peak corresponds to the transformation from the two-phase ($\alpha + \beta$) region of stability to the single-phase β region. An isopleth, or constant-composition section, of the Ti-6Al-4V ternary phase diagram, at 6% Al mass fraction, is shown in Fig. 2 (adapted from Ref. 13) to illustrate this point. Also shown (dashed line) is the V content in this alloy. The 4% V mass fraction line intersects the β-transus around 1280 K, the transformation temperature for this composition. The disagreement of the transformation temperature with the temperature at which the peak in the specific heat curve occurs can be attributed to nonequilibrium structure prior to heating, and the presence of impurities.
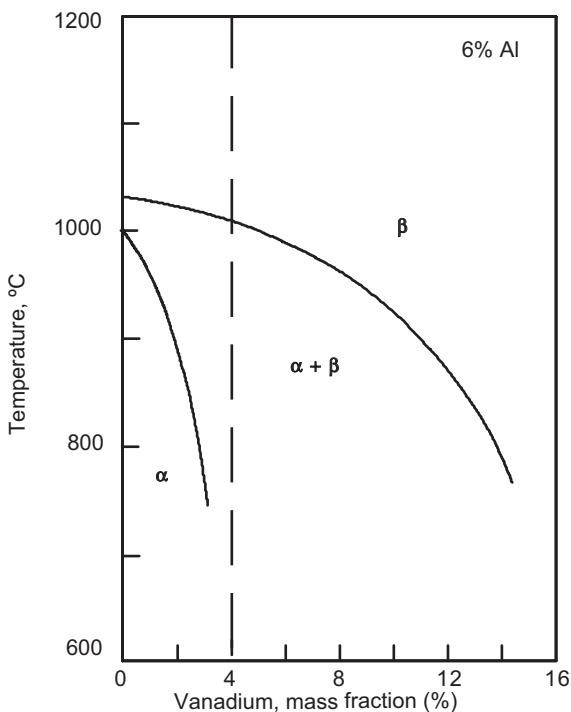
Fig. 2. An isopleth at 6% Al, from the ternary phase diagram for Ti-Al-V, adapted from Ref. 13.

The specific-heat-capacity data for CF8M stainless steel, measured with the intermediate temperature pulse-heating system (Fig. 1), does not show any abrupt changes in slope, indicating single-phase austenite and the absence of phase boundaries in this temperature range.

Figure 3 shows the specific heat capacity in the approximate temperature range of 1400 K to near the melting temperature, determined with the high temperature pulse-heating system for the alloys, IN 718, Ti-6Al-4V, and CF8M stainless steel. For all three materials, the specific heat capacity increases monotonically in this temperature range. For IN 718, the higher slope in the Cp data above 1400 K is probably due the heat absorbed during the dissolution of precipitates still remaining in the microstructure at these temperatures. Brooks et al. have reported two polynomials covering two temperature ranges, to represent IN 718 data measured by adiabatic calorimetry. The slope computed from the polynomial representing Brook et al.'s high temperature data is in good agreement with the slope above 1400 K, of the current work. However, the polynomial does not

Fig. 3. Specific heat capacity versus temperature for Inconel 718, Ti-6Al-4V, and CF8M stainless steel, measured with the high-temperature pulse-heating system.

extend into the range of high-temperature data of the current work, so an extended comparison cannot be made. For Ti-6Al-4V, Cp data above 1400 K is in reasonably good agreement ($< 3\%$ average difference) with data measured by Cezairliyan et al. [10] using a similar system.

4.2. Electrical Resistivity

Figure 4 shows the electrical resistivity of IN 718 and CF8M stainless steel in the approximate temperature range of 350 to 1200 K, determined with the intermediate-temperature pulse-heating system. For IN 718, the electrical resistivity increases gradually up to around 980 K where there is a peak and the values decrease thereafter up to around 1200 K and are mostly constant above this temperature. The peak in the electrical resistivity data corresponds to the sharp rise in the specific-heat data for this material. It is believed that this is due to the dissolution of the precipitates, γ' and γ'', in γ, around the peak temperature. The electrical resistivity of CF8M stainless steel (Fig. 4) shows a gradual rise, increasing by about 50% in this temperature range. Electrical resistivity data from the Auburn University Thermophysical Properties Database are shown (open symbols) alongside the data from the current work, in the temperature range of
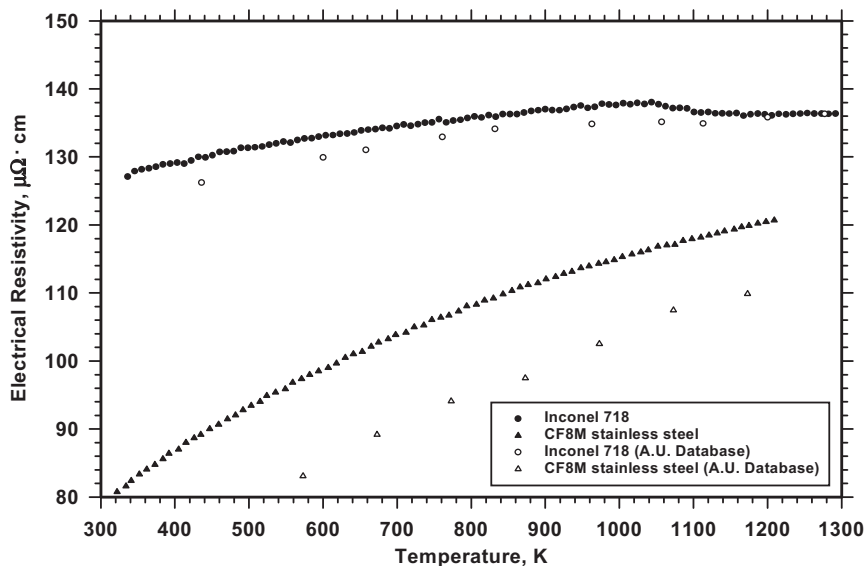
Fig. 4. Electrical resistivity versus temperature for Inconel 718 and CF8M stainless steel, measured with the intermediate-temperature pulse-heating system. Filled symbols represent data from current work. Open symbols represent data calculated from the thermal conductivity using the Wiedemann–Franz–Lorenz Law (W-F-L) law [9].

availability. They have similar trends; the differences are due to the fact that the literature data for the resistivity have been calculated from thermal conductivity data using the Wiedemann–Franz–Lorenz law.

Figure 5 shows the electrical resistivity for the alloys, IN 718, Ti-6Al-4V, and CF8M stainless steel, in the approximate temperature range of 1350 K to near their melting temperatures, determined with the high-temperature pulse-heating system. No phase transformations are identified in this temperature range. The electrical resistivity increases by $< 1\%$ for IN 718 and 2% for Ti-6Al-4V and CF8M stainless steel in this temperature range. For high resistivity alloys, an increase in the thermal disorder ultimately leads to the saturation of the resistivity, thus achieving a minimum conductivity for the alloy system [14], which explains that all three plots in Fig. 5 show small coefficients of electrical resistivity with temperature $(d\rho/dT)$.

5. ESTIMATE OF UNCERTAINTIES

In both the high-temperature and the intermediate-temperature pulse-heating systems, the sources of uncertainty in the specific heat capacity are from the measurement of current, voltage, temperature, and mass, and
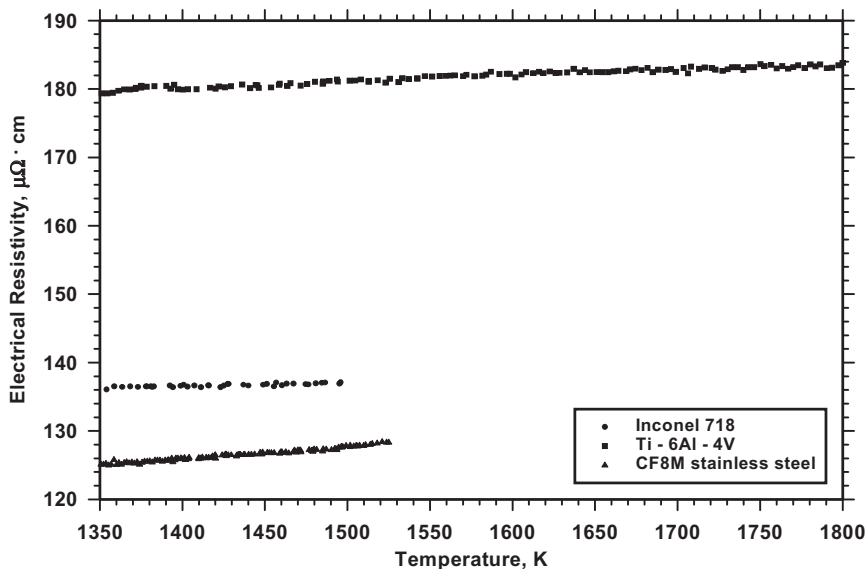
Fig. 5. Electrical resistivity versus temperature for Inconel 718, Ti-6Al-4V, and CF8M stainless steel, measured with the high-temperature pulse-heating system.

from the fitting parameters used to compute and fit the slope of temperature versus time (dT/dt) data. For the electrical resistivity, the sources of error originate in the measurement of the voltage and the current and the knowledge of the corresponding temperature. In the intermediate-temperature system, the temperature measurement uncertainty depends on the calibration error in the thermocouple, whereas in the high-temperature system it depends on the calibration error in the pyrometer as well as that of the ellipsometer which is used to measure the corresponding emissivity. Estimates of uncertainties have been worked out in detail in earlier publications [11, 15]. The expanded uncertainties (two standard deviations) in the resultant properties determined using the high-temperature system are $\pm 3\%$ for specific heat capacity and $\pm 1\%$ for electrical resistivity. For the intermediate-temperature system the corresponding values are $\pm 2\%$ for specific heat capacity and $\pm 1\%$ for electrical resistivity.

6. CONCLUSIONS

Two pulse-heating systems were used to determine the specific heat capacity and electrical resistivity of three industrial alloys from room temperature to their solidus temperatures. Subsecond duration transient experiments are well suited for high-temperature measurements, where

conventional steady-state methods are less reliable because of problems arising out of extended exposure to high temperature, such as, significant heat losses and reactivity with containers. Thermocouple-based, longer duration transient experiments are suitable for the intermediate-temperature range where high-speed pyrometers are not sensitive enough. Data generated from these experiments fill the void for the thermophysical properties of these alloys in certain temperature ranges. The Auburn University Thermophysical Properties Database has been updated with selected data from the current work.

Previously, pulse-heating systems have been used extensively to measure and validate thermophysical-property data for pure metals and binary alloys. The present work extends the technique to multicomponent industrial alloys. Since reliable literature data are not available for the entire temperature range of interest, a thorough validation was not possible. In the range where data were available for comparison, the average absolute deviation in specific heat capacity is about 6% for Inconel 718 and 5% for CF8M stainless steel. The average absolute deviation in the electrical resistivity is about 3% for Inconel 718 and 10% for CF8M stainless steel. It should be noted that the electrical-resistivity literature data are estimated from measurements of thermal conductivity.

For the interpretation of thermophysical-property data measured by high-speed transient techniques, it is desirable that the heat treatment history, phase stability, and the kinetics of transformation of the phases involved, are well understood.

ACKNOWLEDGMENTS

REFERENCES

1. I. Egry, A. Diefenbach, W. Drier, and J. Piller, *Int. J. Thermophys.* **22**:569 (2001).
2. S. Bakhtiyarov and R. Overfelt, *Ann. New York Acad. Sci.*, in press.

3. S. Krishnan, *J. Opt. Soc. Am. A* **9**:1615 (1992).

4. E. Kaschnitz and A. Cezairliyan, *Int. J. Thermophys.* **17**:1069 (1996).

5. A. Cezairliyan, G. M. Foley, M. S. Morse, and A. P. Miiller, in *Temperature–Its Measurement and Control in Science and Industry*, Vol. 6, J. F. Schooley, ed. (AIP, New York, 1992), pp. 757–762.

6. A. Cezairliyan, M. S. Morse, H. A. Berman, and C. W. Beckett, *J. Res. Nat. Bur. Stand. (U.S.) A* **74**:65 (1970).

7. D. Basak, U. R. Kattner, J. L. McClure, D. Josell, and A. Cezairliyan, *Int. J. Thermophys.* **21**:913 (2000).

8. T. Matsumoto, A. Cezairliyan, and D. Basak, *Int. J. Thermophys.* **20**:943 (1999).

9. R. Overfelt and R. Taylor, unpublished research, thermophysical property data available at http://metalcasting.auburn.edu.

10. A. Cezairliyan, L. C. Phillips, J. L. McClure, R. A. Overfelt, C. Matlock, D. Matlock, R. A. McDaniel, A. Giamei, and C. Y. Ho, in *Annual Report: NIST Consortium on Casting of Aerospace Alloys*, p. 95 (1995).

11. D. Basak, Ph.D. dissertation, University of Tennessee, Knoxville (1995).

12. C. R. Brooks, M. Cash, and A. Garcia, *J. Nucl. Mater.* **78**:419 (1978).

13. C. R. Brooks, in *Heat Treatment, Structure and Properties of Nonferrous Alloys* (American Society of Metals, Metals Park, Ohio, 1982), p. 361.

14. P. L. Rossiter, in *The Electrical Resistivity of Metals and Alloys* (Cambridge University Press, Cambridge, 1987), p. 373.

15. A. Cezairliyan, S. Krishnan, and J. L. McClure, *Int. J. Thermophys.* **17**:1455 (1996).